

Effect of Design Features and Operating Conditions on the Performance of a Bipolar Membrane-Based Acid/Base Flow Battery

Andrea Culcasi, Luigi Gurreri*, Alessandro Tamburini, Andrea Cipollina, Giorgio Micale

Dipartimento di Ingegneria, Università degli Studi di Palermo, Viale delle Scienze Ed.6, 90128, Palermo, Italy
luigi.gurreri@unipa.it

In the context of renewable energy sources, storage systems have been proposed as a solution to the issues related to fluctuations in the production and consumption of electric power. The EU funded BAoBaB project is aimed at developing the Acid/Base Flow battery (AB-FB), an environment-friendly, cost-competitive, grid-scale battery storage system based on the cyclic coupling of Bipolar Membrane ElectroDialysis (BMED) and its reverse, the Bipolar Membrane Reverse ElectroDialysis (BMRED) (Pärnamäe et al., 2020). Bipolar membranes promote catalytically water dissociation, thus allowing the storage of electric power in the form of acidic and alkaline solutions (pH gradient), obtained from their corresponding salt (charging mode – BMED), which are then recombined to provide electrical power (discharging mode – BMRED). The membranes are key elements for the process performance; however, the energy conversion efficiency is also affected by the operating parameters of the process and the design features of the stack.

In this work, we performed a sensitivity analysis by a mathematical multi-scale model previously developed (Culcasi et al., 2020a). The performance of AB-FB systems was predicted, focusing on the Round Trip Efficiency. Results showed that proper design features made the effect of parasitic currents negligible. Moreover, proper operating conditions maximized the RTE up to 66%.

1. Introduction

Recently, there has been an increase in the demand for energy from renewable sources (Zappa et al., 2019). However, there is an imbalance between the supply and demand of energy from intermittent sources such as solar and wind. In order to reduce this imbalance, it is necessary to develop storage systems with large capacity, i.e., at the scale of kWh to MWh. These accumulation devices must meet requirements in terms of sustainability and safety, as well as durability and economic affordability. Storage systems can be classified based on the way they store energy (Luo et al., 2015). In recent years, flow batteries, which store energy in the form of electrolyte solutions flowing through them, have been increasing in popularity among the various electrochemical systems (Soloveichik, 2015). Flow batteries are capable of meeting all performance requirements, but currently imply high costs and environmental problems (Díaz-Ramírez et al., 2020).

In this context, the Acid / Base Flow Batteries represent an innovative, safe and sustainable way to accumulate electricity (van Egmond et al., 2018). The AB-FB is an electro-dialytic battery, whose operating principle is based on the water dissociation / recombination reaction performing acid and base production / neutralization (Figure 1). In particular, the Bipolar Membrane ElectroDialysis (BMED) produces acidic and basic solutions during the charging phase (Gurreri et al., 2020). The reverse process, i.e. the Bipolar Membrane Reverse ElectroDialysis (BMRED), uses these solutions in order to generate electricity during the discharging phase (Zaffora et al., 2020). An AB-FB module (stack) consists of several repetitive units called triplets. In turn, a triplet is made up of spacers and ion-exchange membranes. Each spacer occupies the gap between two membranes, thus forming a channel. In a triplet there are three different ion-exchange membranes: the anionic, the cationic and

the bipolar membrane. The bipolar membrane is essentially made up of a cation and an anion exchange layer, one on top of the other (Pärnamäe et al., 2021). Moreover, in the triplet there are three different channels: the acid, base and salt channel.

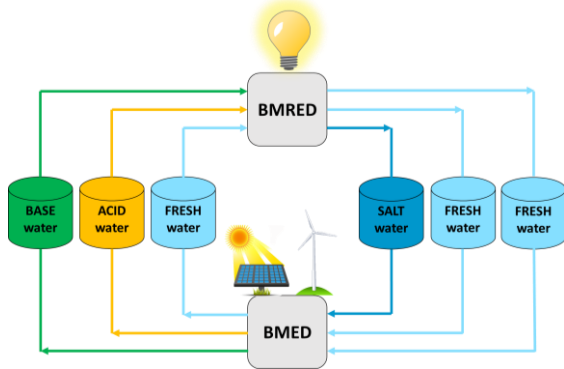


Figure 1: Acid/Base Flow Battery scheme (Culcasi et al., 2020a).

In principle, it is possible to achieve an energy density of $\sim 22 \text{ kWh m}^{-3}$ of one solution when using acid and base solutions at 1 M. However, van Egmond et al. (2018) experimentally measured 5.8 kWh m^{-3} . These energy density values are similar to those typical of the more common Compressed Air Energy Storage systems and Pumped Hydroelectric Systems (4 kWh m^{-3} and 1.3 kWh m^{-3} , respectively). However, the application of these technologies is limited by geographic constraints (Luo et al., 2015). The AB-FB is not affected by these limitations, but presents the drawback of a lower energy density compared to Li-ion or Lead-Acid batteries ($\sim 400 \text{ kWh m}^{-3}$ and $\sim 60 \text{ kWh m}^{-3}$, respectively). Nevertheless, AB-FBs discharge times are in the order of hours rather than minutes.

The AB-FB technology has been poorly studied so far. Kim et al. (2016) observed a constant performance over nine cycles and produced a maximum power density of 2.9 W m^{-2} of total membrane area using a single-cell stack fed with HCl-NaOH solutions at a maximum concentration of 0.7 M.

Using a single-cell unit and 1 M solutions, van Egmond et al. (2018) performed nine cycles, obtaining a power density of the order of 3.7 W m^{-2} . Furthermore, a maximum Round Trip Efficiency of 13.5% along with energy densities of 5.8 kWh m^{-3} (of one solution) was reported. Undesirable protons and hydroxyl ion fluxes resulted in nearly 50% loss of energy, thus causing low coulombic efficiencies, on average 20%. Furthermore, due to high values of stack resistance, the voltage efficiency was relatively low. At high values of current densities, there was the risk of delamination of the bipolar membrane caused by a water diffusion rate lower than the rate of proton and hydroxide recombining. Therefore, the discharge current density was limited to 15 A m^{-2} . Overall, customized membranes with high-performance features are required to achieve higher power densities, as well as process efficiencies.

Likewise, the results presented by Xia et al. (2018) provided similar conclusions with a single-triplet stack operated up to twenty cycles. By testing stacks with up to twenty triplets fed by 1 M solutions, Xia et al. (2020) produced a maximum power density of $\sim 15 \text{ W m}^{-2}$, observing large detrimental effects of parasitic currents via manifolds.

Zaffora et al. (2020) studied the BMRED process under different operating conditions, reporting a maximum power density of 17 W m^{-2} , and estimating an energy density of 10 kWh m^{-3} (1 M HCl-NaOH).

This literature review highlights that it is essential to refine the AB-FBs competitiveness in terms of economic and technological properties. For this purpose, it is crucial to evaluate the battery performance with a comprehensive modelling tool.

In a previous work (Culcasi et al., 2020a) a process model was purposely developed and validated with original experimental data. In the present work, the model was used to study the performance of the AB-FB by a sensitivity analysis to the main operating conditions and to the channel size.

2. Method

Co-ion leakage is recognized as one of the main phenomena that negatively affect the AB-FB performance. However, there are other phenomena occurring at different spatial scales, including ohmic and non-ohmic voltage drops, concentration polarization, pressure drops, and parasitic currents. Unlike pressure drops and concentration polarization (Gurreri et al., 2013), parasitic currents that pass through the collectors and distributors may worsen significantly the performance of AB-FBs, and they typically arise in stacks with a high

number of triplets. An effective simulation tool should simultaneously take into account all of these phenomena, as well as reciprocal influences, when modelling the performance parameters of the battery. The model used for the present simulation analysis was developed by a multi-scale structure and four dimensional scales or levels. The external input of the model is represented by the electrochemical and transport properties of the membranes. This simulation tool allows for studying the performance of the AB-FB module across variations in the stack design (e.g. spacer thickness, spacer length), as well as across different operating conditions (e.g. current density, mean flow velocity). This integrated model was presented in a previous work (Culcasi et al., 2020a) along with a validation with experimental data at various operating conditions. The present simulations regard a batch configuration, where the electrolyte solutions are continuously recirculated into the containers until a target concentration is reached, specifically in terms of the HCl concentration in the acid tank.

The results that will be shown in the next section, refer to the Round Trip Efficiency, calculated as follows,

$$RTE = CE \times VE = \frac{\int_0^{t_d} I_{ext,d} U_{ext,d} dt}{\int_0^{t_c} I_{ext,c} U_{ext,c} dt} \quad (1)$$

where CE and VE are the Coulombic Efficiency and the Voltage Efficiency, respectively, I_{ext} is the electric current in the external circuit, U_{ext} is the external voltage, which coincides with the stack voltage, t is the process time, and the subscripts c and d refer to charge and discharge, respectively.

Coulombic Efficiency and Voltage Efficiency are calculated as

$$CE = \frac{\int_0^{t_d} I_{ext,d} dt}{\int_0^{t_c} I_{ext,c} dt} \quad (2)$$

$$VE = \frac{t_c \int_0^{t_d} U_{ext,d} dt}{t_d \int_0^{t_c} U_{ext,c} dt} \quad (3)$$

The Round Trip Efficiency is a useful figure of merit of the energy storage devices. Indeed, it accounts for both the energy collected during the discharge phase and the energy provided to the system during the charge phase. An ideal storage device with 100% of RTE would provide in discharge the same amount of energy that was consumed in charge. However, due to internal losses, there is an imbalance between the energy collected during the discharge and the energy input during the charge, which leads to a decrease in the RTE. For example, the most commonly used storage technologies, such as Compressed Air Energy Storage (CAES) or Pumped Hydro Storage (PHS), have RTE values within the ranges 42-89% and 65-85%, respectively (Bullich-Massagué et al., 2020).

Moreover, in order to evaluate the impact of the parasitic currents via the manifolds, the loss of RTE (RTE_{lost}) with respect to the ideal case without parasitic currents was calculated:

$$RTE_{lost} = RTE_{no\ par} - RTE \quad (4)$$

in which $RTE_{no\ par}$ is the RTE computed by using a simplified model, which neglects parasitic currents.

The storage capacity of the AB-FB is given by the volumes and concentrations of the electrolytes. The present simulations were performed with the initial acid ($V_{t,a}$), base ($V_{t,b}$) and salt ($V_{t,s}$) volumes calculated as follows:

$$V_{t,a} = V_{t,b} = \frac{L \times b}{0.476 \times 0.44} 0.01 \quad (5)$$

$$V_{t,s} = 6 \times V_{t,a} \quad (6)$$

in which L and b are the spacer length and width, respectively. $V_{t,a}$ and $V_{t,b}$ (m^3 , Eq. 5) were related to the reference length and width, and corrected according to the actual length and width (see Table 1). $V_{t,s}$ (Eq. 6) has been chosen in order to satisfy a fixed volumes ratio $V_{t,a} : V_{t,b} : V_{t,s}$ equal to 1:1:6.

Table 1 shows the input parameters used for the present sensitivity analysis. The simulations were performed by varying both the operating and design parameters of the process, whilst running single cycles of the battery. The simulations were performed with a stack design that reduces pressure drops. Moreover, parasitic currents through the manifolds are expected to be negligible because of the low number of triplets used as well as the low value of the manifolds area (Culcasi et al., 2020b), i.e. a single rectangular hole of $400\ mm^2$. The fixed or reference values of the present simulations correspond to the features of the AB-FB pilot plant of the EU funded BAoBaB project (Pärnamäe et al., 2020). The stack is composed by 8 blocks, each with 7 triplets. A single 7-triplet block was simulated because each of them is a repetitive unit. The electrode compartments were simply simulated as ohmic elements by a blank resistance, including the contribution of the end-membrane (i.e. AEM), evaluated experimentally.

Table 1: Input of the multi-scale model for the sensitivity analysis.

| Membrane properties | | | | |
|--|----------------------------|-----------------------|-----------------------|-----|
| | units | AEM | CEM | BPM |
| Thickness | μm | 75 | 75 | 120 |
| Areal resistance | $\Omega\text{ cm}^2$ | 4 | 3.5 | 5 |
| H ⁺ diffusivity | $\text{m}^2\text{ s}^{-1}$ | 2×10^{-11} | 0.7×10^{-11} | - |
| Na ⁺ diffusivity | $\text{m}^2\text{ s}^{-1}$ | 1.6×10^{-11} | 0.5×10^{-11} | - |
| OH ⁻ diffusivity | $\text{m}^2\text{ s}^{-1}$ | 1.9×10^{-11} | 0.6×10^{-11} | - |
| Cl ⁻ diffusivity | $\text{m}^2\text{ s}^{-1}$ | 1.7×10^{-11} | 0.6×10^{-11} | - |
| Fixed charge group | mol m^{-3} | 5,000 | 5,000 | - |
| Design parameters | | | | |
| | units | fixed/reference | variable | |
| Number of triplets | - | 7 | | |
| Spacer length, L | m | 0.44 | 0.1-0.5 | |
| Spacer width, b | m | 0.476 | | |
| Spacer thickness, H | μm | 475 | 300-700 | |
| Manifold area | mm^2 | 400 | | |
| Operating conditions at the beginning of the charge | | | | |
| HCl concentration in the acid tank | mol m^{-3} | 50 | | |
| NaCl concentration in the acid tank | mol m^{-3} | 250 | | |
| HCl concentration in the salt tank | mol m^{-3} | 10 | | |
| NaCl concentration in the salt tank | mol m^{-3} | 500 | | |
| NaOH concentration in the base tank | mol m^{-3} | 50 | | |
| NaCl concentration in the base tank | mol m^{-3} | 250 | | |
| Target concentrations and fluid velocity | | | | |
| HCl target at the end of the charge | mol m^{-3} | 1000 | 600-1000 | |
| HCl target at the end of the discharge | mol m^{-3} | 50 | 50-400 | |
| Mean flow velocity during charge | cm s^{-1} | 0.5 | 0.5-5 | |
| Mean flow velocity during discharge | cm s^{-1} | 0.5 | 0.5-5 | |
| Electrode compartments and external electric circuit | | | | |
| Blank resistance | $\Omega\text{ cm}^2$ | 12 | | |
| Charge current density | A m^{-2} | 100 | 100-170 | |
| Discharge current density | A m^{-2} | 30 | 30-130 | |

3. Results and discussion

The first analysis was conducted by allowing the charge / discharge external current to vary (Figure 2).

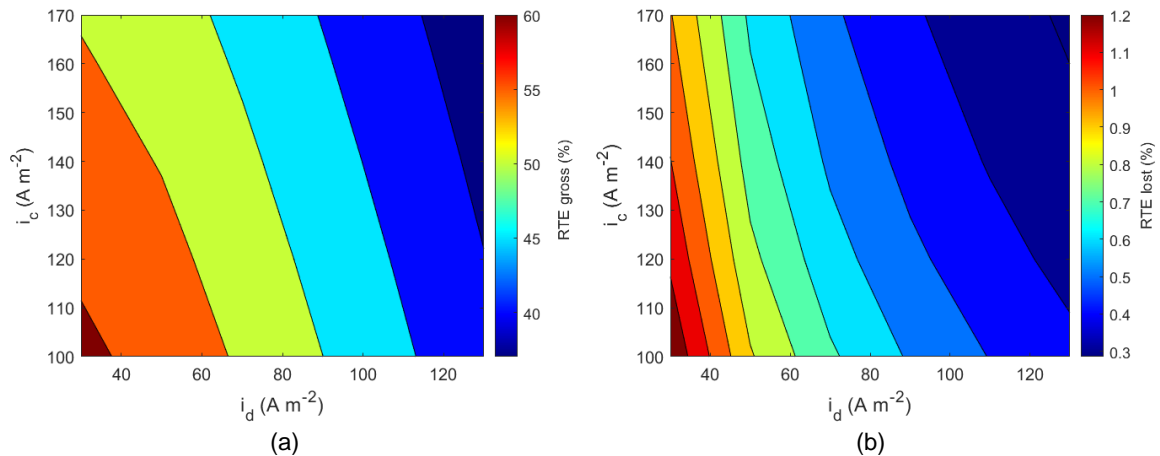


Figure 2: Contour maps of the Round Trip Efficiency a), and of the loss of Round Trip Efficiency due to parasitic currents b) as functions of the charge and discharge external current densities.

As shown by the contour map in Figure 2a, the RTE values decrease with increasing charge and discharge external current densities. Particularly, RTE ranges between 38% and 60%. As the current density increases, the Coulombic Efficiency increases, but the Voltage Efficiency decreases more markedly, thus leading to a reduction in RTE. The maximum RTE was found to be close to the origin of this contour map. Therefore, lower current densities should be considered to maximize the RTE. However, low values of current density in discharge would provide low values of power density.

As reported in Figure 2b, the RTE loss due to parasitic currents is mostly less than 1%, thus proving the negligible effect of shortcut currents using the present battery design.

The effect of fluid velocity and target concentration is reported in Figure 3.

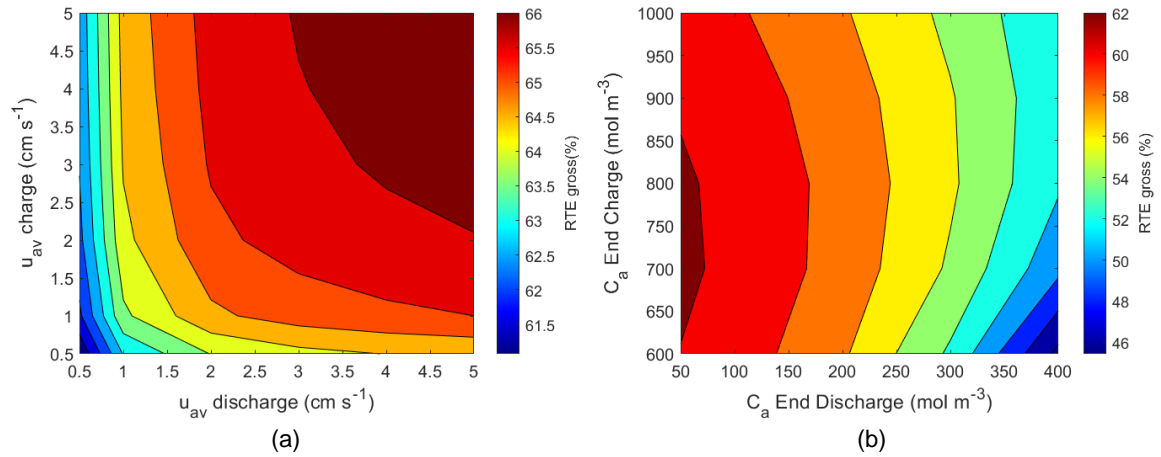


Figure 3: Contour maps of the Round Trip Efficiency as functions of a) the charge and discharge mean flow velocity and b) HCl concentration in the acid tank at the end of charge and discharge.

As shown in Figure 3a, the higher the mean flow velocities, the higher the Round Trip Efficiency, with more significant effects due to the fluid velocity in the discharge phase. However, by increasing the mean flow velocities for both charge and discharge from 0.5 to 5 cm s⁻¹, the highest increase of RTE is low (5%). This is due to a double effect. On one side, the relative increase of the discharge over the charge time, and on the other side, the relative increase of the average power density of the discharge over that of the charge. The RTE is less sensitive to the fluid velocity (Figure 3a) than to the current density (Figure 2). Moreover, the increase of gross RTE should be weighed up against the increase of pumping power which, in turn, will affect the net RTE. However, the stack design considered here was found to have low values of pressure drops, which were estimated to be within the range 0.03%-3.3% of RTE, thus making their effect on the battery performance negligible. In Figure 3b, the effect of using different concentrations is shown. Particularly, different target concentrations at the end of the charge and discharge were set. It was observed that the higher the discharge target, the lower the RTE. Specifically, there is a sharp drop of ~10% of RTE by increasing the concentration from 50 mol m⁻³ to 400 mol m⁻³. This is mainly due to the reduction of the Coulombic Efficiency when increasing the average concentration of the discharge. In contrast, by keeping the discharge target concentration constant, there is an initial increase of the RTE when increasing the target concentration of the charge, then followed by a decrease of RTE. However, the effects of the charge target concentration are smaller. Overall, the variation of RTE is slightly lower than that observed by changing the current density. A maximum RTE of 62.4% was obtained at target concentrations of 50 mol m⁻³ and ~700 mol m⁻³ for the discharge and charge, respectively.

Two design parameters were also studied, which are the spacer thickness and the channel length. Regarding the thickness of the spacer, the simulation analysis revealed that, in the range between 300 μm and 700 μm , the RTE remained almost unchanged. Instead, the effects due to channel length were significant. In fact, by increasing the length from 0.1 m to 0.5 m, an increase in RTE from ~46% to ~61% was obtained. As the channel length increased, there was no appreciable variation in Voltage Efficiency. However, a significant increase in Coulombic Efficiency was observed, thus leading to an increase in RTE. The increase in Coulombic Efficiency can be attributed to the indirect effect of the increase in the tank volume with the longer length of the channel, as shown in Equation 5. Therefore, in relative terms, there was a greater increase in the discharge time compared to the charge time, which thus enhanced the Coulombic Efficiency, as mentioned above.

4. Conclusions

In this work, the performance of an Acid/Base Flow battery was investigated by a sensitivity analysis conducted by a process model. The choice of proper operating conditions and design features allows better performance in terms of Round Trip Efficiency. In the present simulations, parasitic currents via manifolds were found to be negligible, as they accounted for a loss of RTE less than 1%, thanks to suitable geometrical features (low number of triplets and small manifold area). Among the operating conditions, the RTE was more sensitive to the current density and, to a slightly lesser extent, to the target concentrations. Instead, much smaller effects were due to the fluid velocity. Overall, a maximum RTE of 60-66% was obtained by changing the operating conditions. Regarding the design features of the stack, the spacer thickness had only minor effects on the RTE, while the channel length enhanced the RTE from 46% to 61% when increasing from 0.1 m to 0.5 m. Future developments of the AB-FB technology can be pursued by larger and more detailed analyses, including optimization studies.

Acknowledgments

This work was performed in the framework of the BAoBaB project (Blue Acid/Base Battery: Storage and recovery of renewable electrical energy by reversible salt water dissociation). The BAoBaB project has received funding from the European Union's Horizon 2020 Research and Innovation program under Grant Agreement no. 731187 (www.baobabproject.eu).

References

- Bullich-Massagué E., Cifuentes-García F.J., Glenny-Crende I., Cheah-Mañé M., Aragüés-Peñalba M., Díaz-González F., and Gomis-Bellmunt O., 2020, A Review of Energy Storage Technologies for Large Scale Photovoltaic Power Plants, *Applied Energy*, 274, 115213.
- Culcasi A., Gurreri L., Zaffora A., Cosenza A., Tamburini A., and Micale G., 2020a, On the Modelling of an Acid/Base Flow Battery: An Innovative Electrical Energy Storage Device Based on pH and Salinity Gradients, *Applied Energy*, 277, 115576.
- Culcasi A., Gurreri L., Zaffora A., Cosenza A., Tamburini A., Cipollina A., and Micale G., 2020b, Ionic Shortcut Currents via Manifolds in Reverse Electrodialysis Stacks, *Desalination*, 485, 114450.
- Díaz-Ramírez M.C., Ferreira V.J., García-Armingol T., López-Sabirón A.M., and Ferreira G., 2020, Environmental Assessment of Electrochemical Energy Storage Device Manufacturing to Identify Drivers for Attaining Goals of Sustainable Materials 4.0, *Sustainability*, 12, 342.
- van Egmond W. J., Saakes M., Noor I., Porada S., Buisman C. J. N., and Hamelers H. V. M., 2018, Performance of an Environmentally Benign Acid Base Flow Battery at High Energy Density, *International Journal of Energy Research*, 42, 1524–1535.
- Gurreri L., Tamburini A., Cipollina A., Micale G. and Ciofalo M., 2013, CFD Simulation of Mass Transfer Phenomena in Spacer Filled Channels for Reverse Electrodialysis Applications, *Chemical Engineering Transactions*, 32, 1879-1884.
- Gurreri L., Tamburini A., Cipollina A., and Micale G., 2020, Electrodialysis Applications in Wastewater Treatments for Environmental Protection and Resources Recovery: A Systematic Review on Progress and Perspectives, *Membranes*, 10, 146.
- Kim J.H., Lee J.H., Maurya S., Shin S.H., Lee J.Y., Chang I.S., and Moon S.H., 2016, Proof-of-Concept Experiments of an Acid-Base Junction Flow Battery by Reverse Bipolar Electrodialysis for an Energy Conversion System, *Electrochemistry Communications*, 72, 157–161.
- Luo X., Wang J., Dooner M., and Clarke J., 2015, Overview of Current Development in Electrical Energy Storage Technologies and the Application Potential in Power System Operation, *Applied Energy*, 137, 511–536.
- Pärnamäe R., Gurreri L., Post J., van Egmond W.J., Culcasi A., Saakes M., Cen J., Goosen E., Tamburini A., Vermaas D.A., and Tedesco M., 2020, The Acid-Base Flow Battery: Sustainable Energy Storage via Reversible Water Dissociation with Bipolar Membranes, *Membranes*, 10, 409.
- Pärnamäe R., Mareev S., Nikonenko V., Melnikov S., Sheldeshov N., Zabolotskii V., Hamelers H. V. M., and Tedesco M., 2021, Bipolar Membranes: A Review on Principles, Latest Developments, and Applications, *Journal of Membrane Science*, 617, 118538.
- Soloveichik G.L., 2015, Flow Batteries: Current Status and Trends, *Chemical Reviews*, 115, 11533–11558.
- Xia J., Eigenberger G., Strathmann H., and Nieken U., 2018, Flow Battery Based on Reverse Electrodialysis with Bipolar Membranes: Single Cell Experiments, *Journal of Membrane Science*, 565, 157–168.
- Xia J., Eigenberger G., Strathmann H., and Nieken U., 2020, Acid-Base Flow Battery, Based on Reverse Electrodialysis with Bi-Polar Membranes: Stack Experiments, *Processes* 8, 99.
- Zaffora A., Culcasi A., Gurreri L., Cosenza A., Tamburini A., Santamaria M., and Micale G., 2020, Energy Harvesting by Waste Acid/Base Neutralization via Bipolar Membrane Reverse Electrodialysis, *Energies* 13, 5510.
- Zappa W., Junginger M., and van den Broek M., 2019, Is a 100% Renewable European Power System Feasible by 2050?, *Applied Energy*, 233–234, 1027–1050.